NASA TECHNICAL MEMORANDUM

NASA TM X-1261

ORIGIN OF HIGH-INTENSITY NOISE IN THE AREA OF A LARGE PROTUBERANCE ON A LAUNCH VEHICLE

by Michael L. Nacht and Raymond A. Turk

Lewis Research Center
Cleveland, Ohio

NATIONAL AERONAUTICS AND SPACE ADMINISTRATION • WASHINGTON, D. C. • JULY 1966

NASA TM X-1261

ORIGIN OF HIGH-INTENSITY NOISE IN THE AREA OF A LARGE PROTUBERANCE ON A LAUNCH VEHICLE

By Michael L. Nacht and Raymond A. Turk

Lewis Research Center
Cleveland, Ohio

NATIONAL AERONAUTICS AND SPACE ADMINISTRATION

For sale by the Clearinghouse for Federal Scientific and Technical Information
Springfield, Virginia 22151 – Price $1.00

ORIGIN OF HIGH-INTENSITY NOISE IN THE AREA OF A LARGE PROTUBERANCE ON A LAUNCH VEHICLE

by Michael L. Nacht and Raymond A. Turk

Lewis Research Center

SUMMARY

A 1/10-scale Atlas-Agena-Mariner C was tested in the Lewis 10- by 10-foot wind tunnel over a Mach number range of 2.0 to 2.5 at an angle of attack of 0°. Attention was centered on the fluctuating pressure activity in the area of an equipment pod. Power-spectral-density analyses failed to reveal distinct power spectra levels at model frequencies corresponding to full-scale frequencies where significant power concentrations had been observed. This indicates the possibility that these large flight vibratory levels may be caused by pressure fluctuations that excite vehicle structures at their natural resonant frequencies. Root-mean-square fluctuating pressure studies revealed that flow separation and shock - boundary-layer interaction may contribute significantly to the general level of pressure fluctuations on launch vehicles.

INTRODUCTION

High-intensity vibrational effects experienced by launch vehicles have emerged as a significant problem area in recent space missions. Examination of data from recent Atlas flights (ref. 1) reveals that considerable vibration activity was imposed on launch vehicle guidance equipment in an external pod over a Mach number range of 2.0 to 2.5. Furthermore, power-spectral-density analyses of flight acceleration measurements indicate relatively high power concentrations at distinct response frequencies. Reference 1 indicates that specific power-spectral-density peaks were observed at 600 and 900 cps with a 50 cps bandwidth resolution. The present wind tunnel program was conducted to ascertain if these disturbances had an aerodynamic origin and to determine boundary-layer effects on the frequency and amplitude of the resulting measured pressure fluctuations.

A 1/10-scale Atlas-Agena-Mariner C was tested in the Lewis 10- by 10-foot super-

sonic wind tunnel with Mach number, dynamic pressure, and altitude as the primary test variables. Both the original model and a configuration with a redesigned pod were investigated. Dynamic pressure transducers were used to measure pressure fluctuations in the pod area. From the transducer data, root-mean-square differential-pressure-coefficient values and power-spectral-density variations were obtained for the areas of greatest activity. In addition, the effect of boundary layer on pressure fluctuations was examined.

SYMBOLS

$\Delta C_p(rms)$	root-mean-square differential pressure coefficient
D	characteristic dimension
f	frequency, cps
M_0	Mach number
Re	Reynolds number
u/U_0	boundary-layer velocity ratio
V	velocity, ft/sec
y/δ	boundary-layer distance ratio
φ	power spectral density, $(lb/sq\ ft)^2/cps$
δ/X	boundary-layer thickness ratio
Subscripts:	
fs	full scale
m	model

APPARATUS AND PROCEDURE

Testing was conducted at free-stream Mach 2.0 to 2.5 and at an angle of attack of 0^o. Dynamic pressures decreased from 530 pounds per square foot at Mach 2.0 to 490 pounds per square foot at Mach 2.5, while the Reynolds number per foot remained constant at 2.55×10^6. Similitude of wind tunnel altitude with flight trajectory was maintained within 12 000 feet over the range of Mach numbers tested.

Figure 1 shows the full-length model installed in the 10- by 10-foot supersonic wind

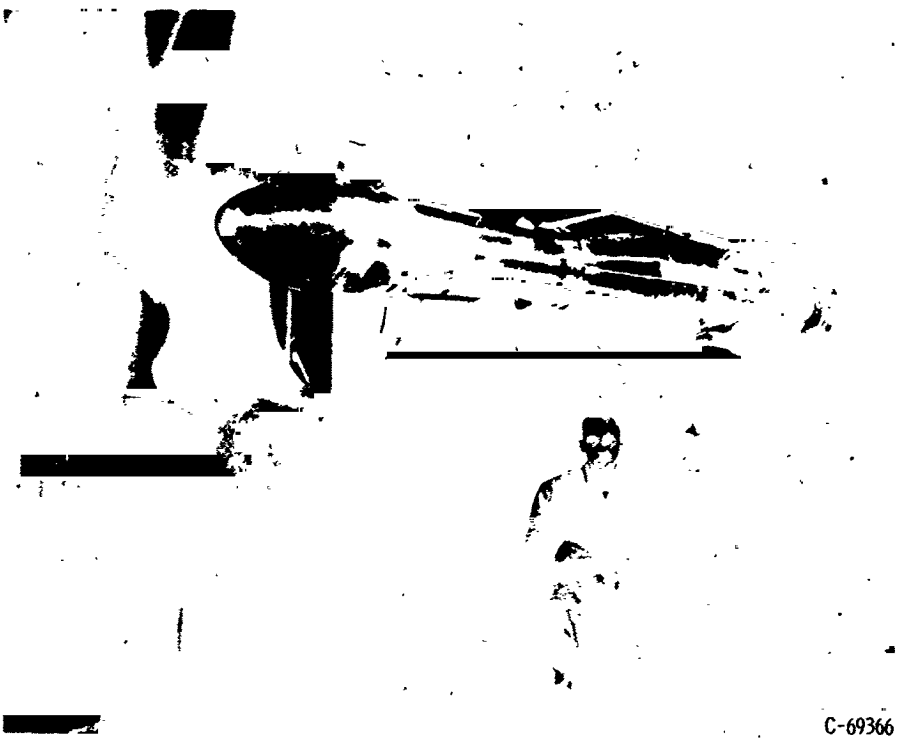

Figure 1. - Full-length model installed in 10- by 10-foot supersonic wind tunnel.

tunnel. The Atlas-Agena-Mariner C configuration was sting mounted in the tunnel. Additional configurations, which will be described herein, were also mounted in this manner.

Frequently, wind tunnel models are characterized by boundary-layer thicknesses in excess of values dictated by their corresponding full-scale vehicles. In order to study boundary-layer effects on pressure fluctuations, a 1/10-scale Atlas short-nose configuration was tested along with the 1/10-scale Atlas-Agena-Mariner C. A schematic drawing of the full-length and shortened models appears in figure 2. The shortened model measured 53.0 inches in length from the model tip to the start of the equipment pod compared with 90.0 inches for the full-length model. The shortened model correctly simulated flat-plate theory estimates of the boundary-layer-thickness characteristics of the full-scale vehicle at the equipment pod.

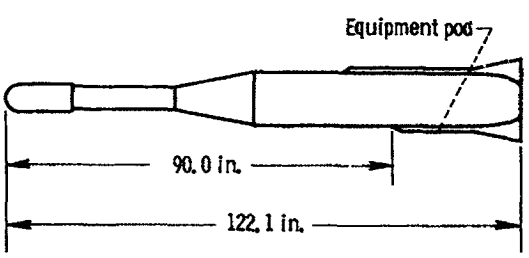

(a) Full-length model A of Atlas-Agena-Mariner C.

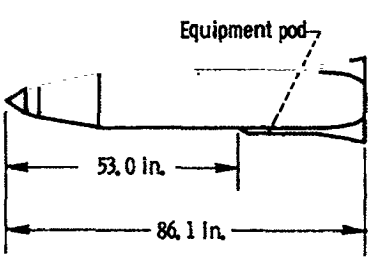

(b) Shortened model of short-nose Atlas.

Figure 2. - Schematic of full-length and shortened models. Scale, 1/10.

Modifications of the original pod included the reduction of the pod wedge half-angle from 26° to 15° and the extension of the pod length from 16.39 to 19.86 inches. These alterations of length and wedge angle are illustrated in figure 3, which shows the forward segments of the original and

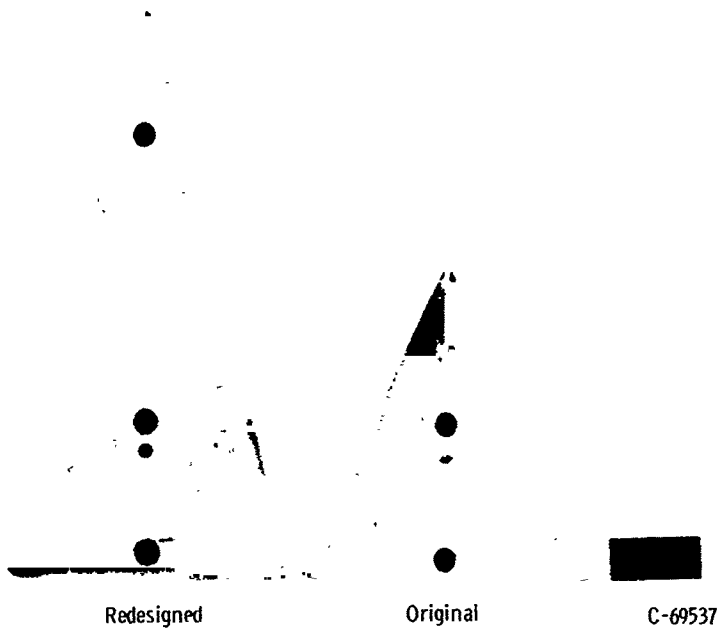

Figure 3. - Forward segments of redesigned and original pods showing length and wedge angle modifications.

Figure 4. - Original equipment pod with installed pressure transducers.

redesigned pods. Both pods were extensively instrumented. Figure 4 shows the original equipment pod with installed pressure transducers. Details of the transducer locations in the pod area for the original and redesigned pods are presented in figure 5. A total of 15 high-frequency pressure transducers were installed on and adjacent to the pod so that the effect of flow disturbances on the pod area could be studied. Transducers 13 and 16 were relocated to positions 13-A and 16-A when the redesigned pod replaced the original.

Figure 6 is a block diagram of the dynamic pressure data measurement system. Because of the long cable lengths that are necessary for testing, a low-noise coaxial cable was used to maintain a high signal-to-noise ratio. The pressure transducers had a range that extended from 0 to 3000 pounds per square inch with a rating of 1 percent linearity. They could tolerate temperatures from -400° to 500° F and were acceleration sensitive to 0.01 pound per square inch per g. The small size of this transducer (0.218-in. diam) was advantageous because it permitted the flush mounting that was necessary for high frequency response. It should be noted further that the data recording equipment had a frequency response from 0 to 20 kcps with an accuracy of ±0.5 decibel.

The dynamic-pressure data reduction system is indicated by a block diagram in figure 7. The root-mean-square voltmeter had a frequency range of 10 cps to 10 Mcps. It had an accuracy rating of ±5 percent from 10 to 50 cps and ±1 percent from 50 cps to 10 Mcps. The power-spectral-density analyzer displayed and plotted, on its associated recorder, the relative total voltage or power as a function of frequency characteristics of a selected spectrum segment. The data reduction equipment for power-spectral-density analysis had a frequency range of 5 cps to 22.5 kcps with an amplitude accuracy of ±7 percent. The bandwidth resolution used for this analysis was 50 cps.

RESULTS AND DISCUSSION

Before the power-spectral-density measurements are discussed, it is pertinent to evaluate the boundary-layer characteristics in the pod area. The boundary-layer thickness variation for the tested configuration is presented as a function of Mach number in figure 8. Boundary-layer thickness divided by pod height is plotted against Mach number for the 1/10-scale Atlas-Agena-Mariner C, the 1/10-scale Atlas short-nose configuration, and the full-scale Atlas-Agena-Mariner C. The original pod was used for both model configurations in figure 8. The figure indicates that the 1/10-scale Atlas-Agena-Mariner C configuration experienced a boundary layer that completely immersed the equipment pod at all Mach numbers tested. In contrast, the boundary-layer thickness of the short-nose configuration barely exceeded half the pod height for Mach 2.0 to 2.5. The short-nose boundary-layer thickness was in close agreement with results calculated

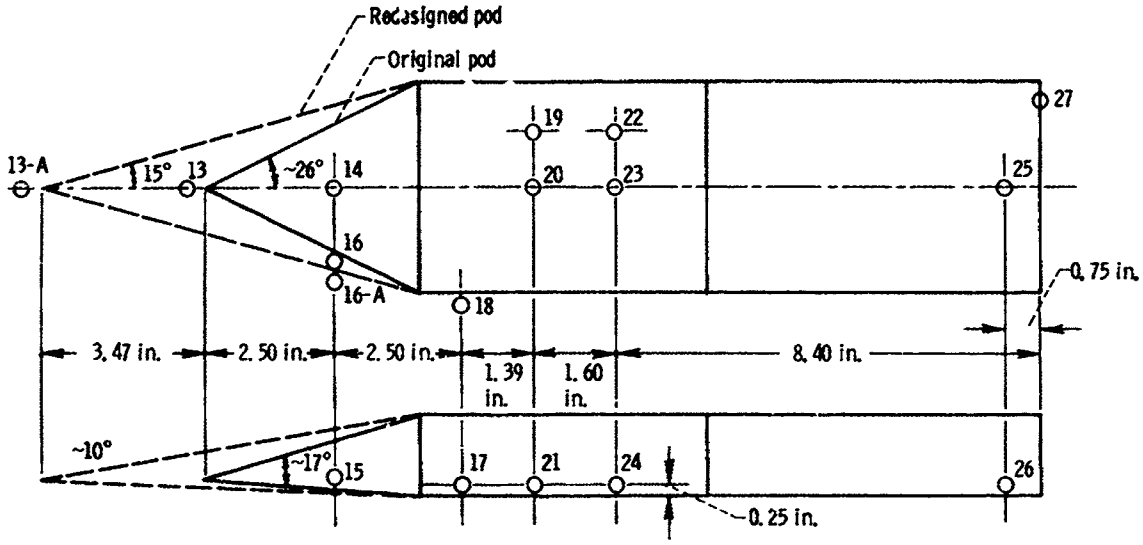

Figure 5. - Transducer locations in pod area for original and redesigned pods.

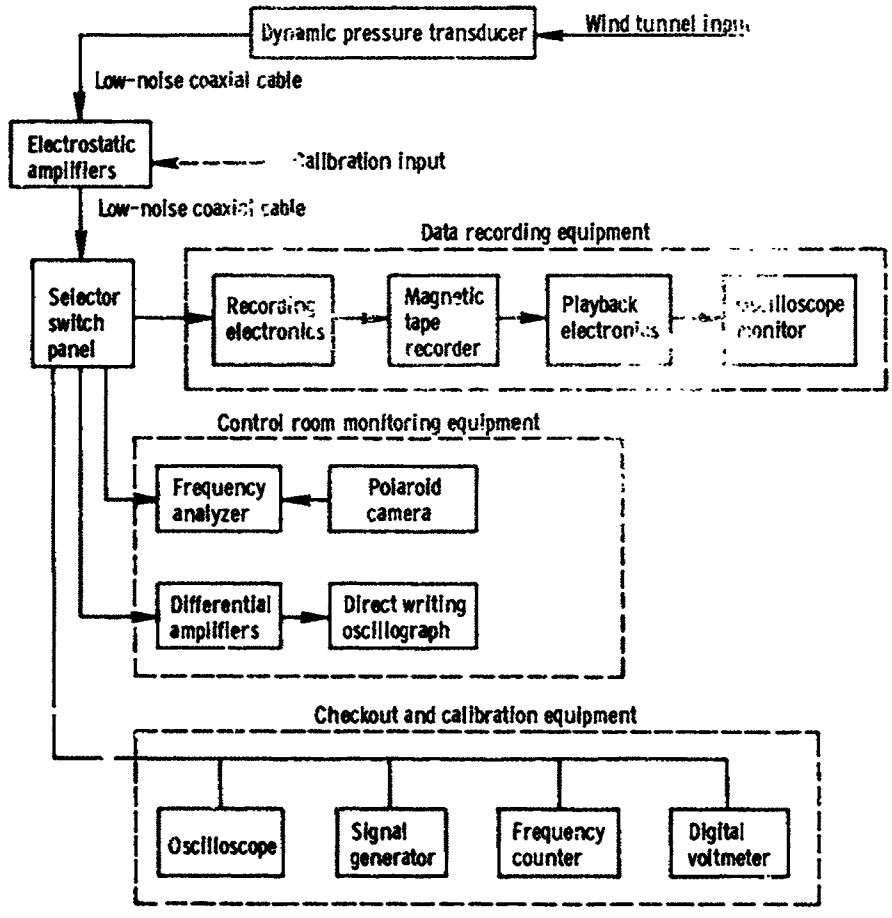

Figure 6. - Dynamic pressure data measurement system.

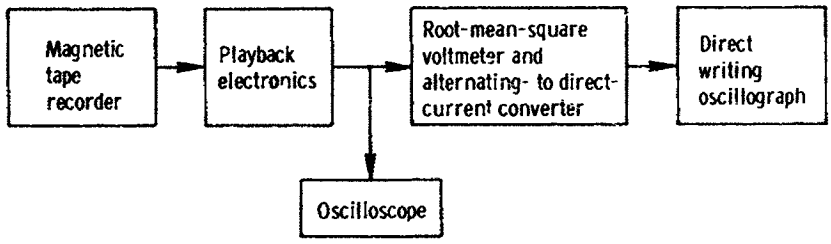

(a) Root-mean-square data reduction.

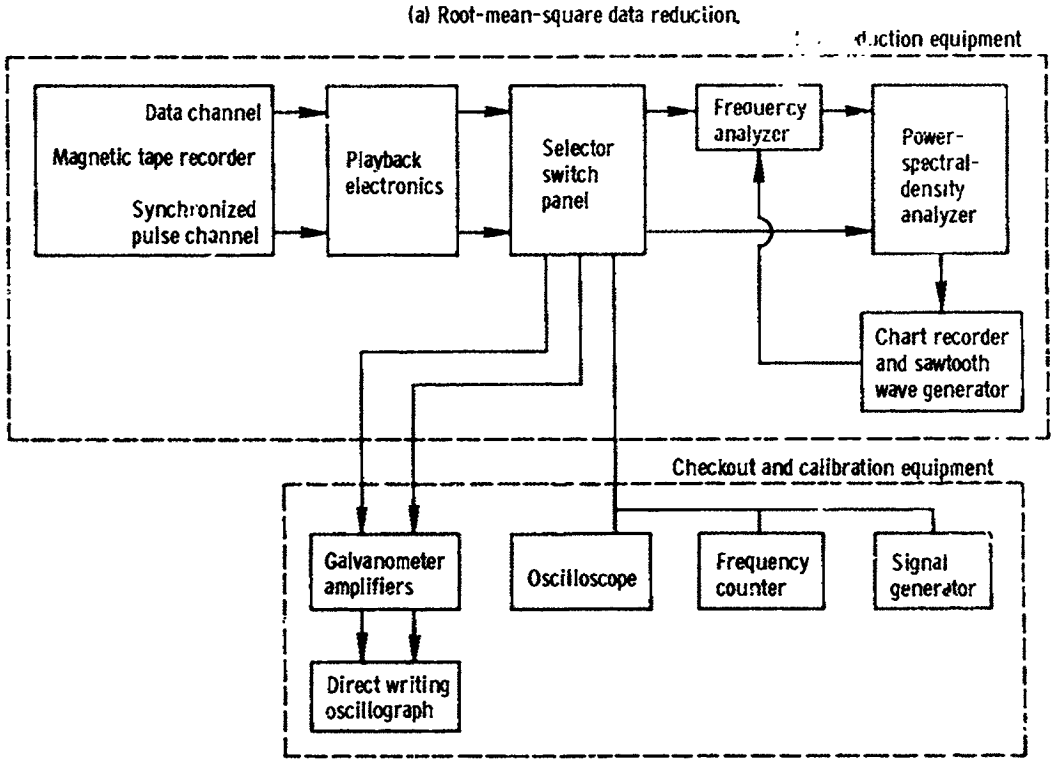

(b) Power-spectral-density analysis.

Figure 7. - Dynamic pressure data reduction system.

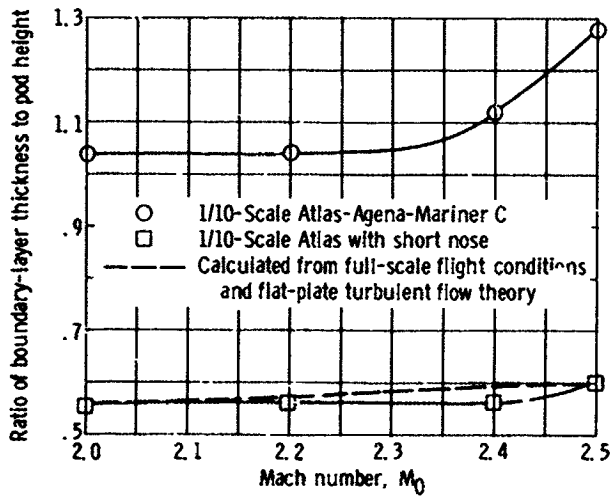

Figure 8 - Boundary-layer thickness variation for tested configurations.

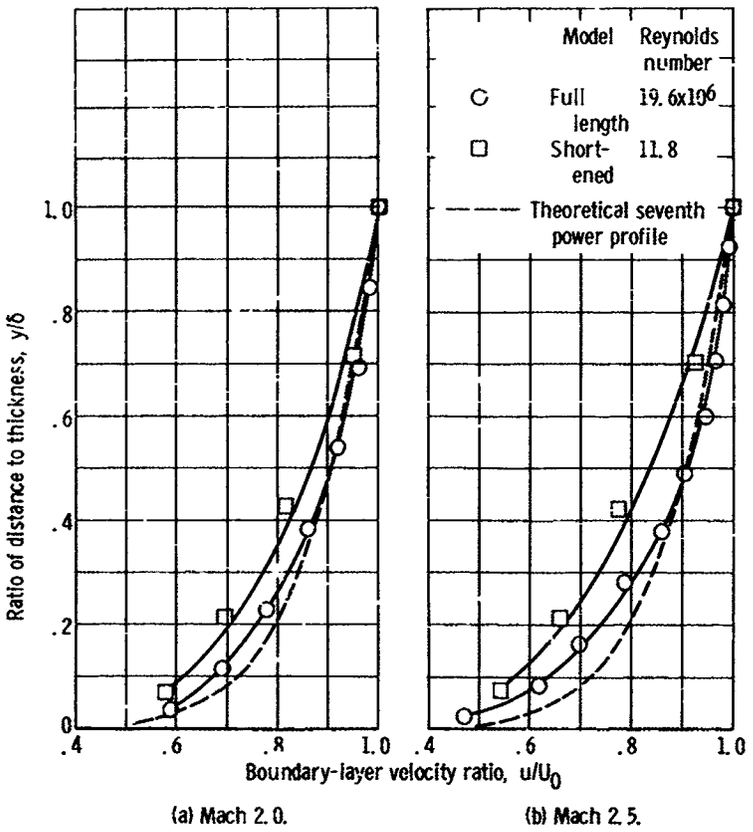

Figure 9. - Comparison of boundary-layer profiles for tested configurations.

from full-scale flight conditions and flat-plate turbulent flow theory described by

$$\frac{\delta}{X} = 0.376\ Re^{-1/5}$$

Another configuration-dependent characteristic was boundary-layer profile. The boundary-layer profiles for the full-length and shortened models were plotted in figure 9 in the conventional form of the ratio of distance to thickness y/δ as a function of boundary-layer velocity ratio u/U_0. The Reynolds number that corresponded to the profile of the full-length model was 19.6×10^6, while the corresponding Reynolds number for the shortened model was 11.8×10^6. Comparisons were made at Mach 2.0 and 2.5, and the theoretical seventh-power profile of turbulent flow was included at both conditions. It was observed that the boundary-layer profile of the shortened model was considerably flatter than either the full-length model profile or the theoretical profile. It should be noted that figure 8 illustrates that the shortened model was introduced to simulate more closely full-scale boundary-layer-thickness characteristics. Figure 9, however, indicates that a modified boundary-layer profile also resulted.

The variation of root-mean-square fluctuating pressures in the equipment pod area (over the entire frequency range) is presented in figure 10 as a function of Mach number.

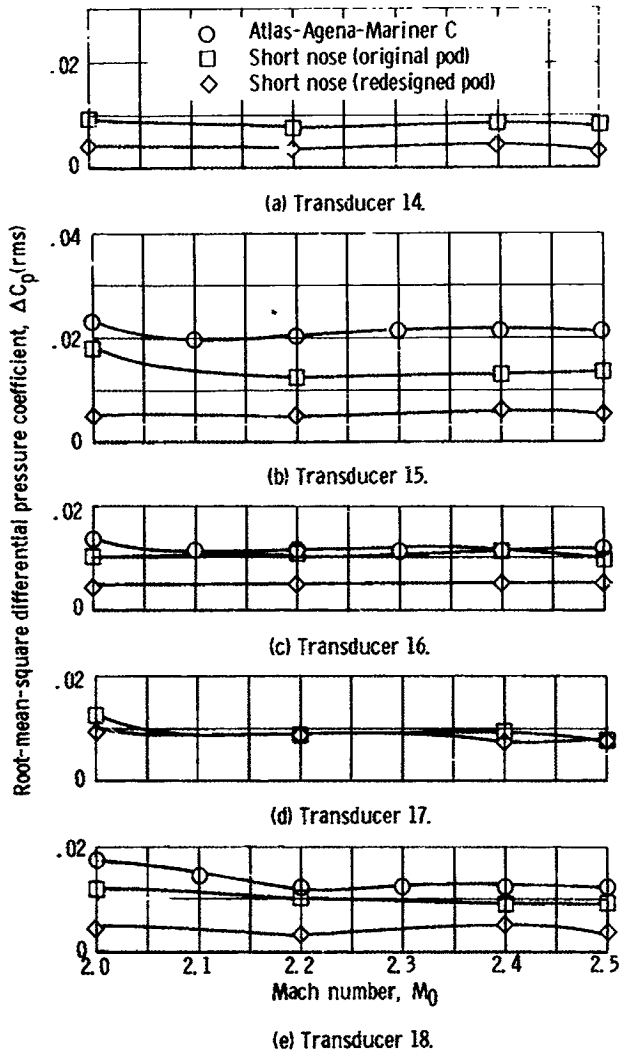

(a) Transducer 14.

(b) Transducer 15.

(c) Transducer 16.

(d) Transducer 17.

(e) Transducer 18.

Figure 10. - Fluctuating pressures in pod area.

Control-room monitoring equipment indicated that transducers 14 to 18 (see fig. 5, p. 6) were the most active of the transducers installed in the pod area. Transducer 15, located on the side of the forward segment of both the original and redesigned pods, showed the greatest activity. In order to determine true values of fluctuating pressures, it was necessary to recognize the contribution made by electrical noise with the tunnel down. This was achieved by the simple relation

$$\left[\Delta C_p(\text{rms})\right] = \sqrt{\left[\Delta C_p(\text{rms})\right]^2_{\text{wind on}} - \left[\Delta C_p(\text{rms})\right]^2_{\text{tunnel down}}}$$

A number of trends were indicated by the transducer data. The values of ΔC_p(rms) ranged from 0.0038 to 0.0235 with most of them between 0.004 and 0.012. There was a relatively slight variation of ΔC_p(rms) levels over the Mach range investigated for each of the three configurations examined. The use of a short nose in place of the Agena-

Mariner C reduced the fluctuating pressures considerably (by as much as 40 percent for transducer 15). It is felt that reduction of shock - boundary-layer interaction because of modifications of the boundary-layer profile and thickness may have caused these lower fluctuating pressure levels. The redesigned pod tested with the short nose indicated a further substantial decrease in fluctuating pressure activity compared with the short-nose - original pod combination (70 percent reduction at Mach 2.0 for transducer 15). The original pod was characterized by a detached oblique shock wave at the forward tip, which caused substantial shock - boundary-layer interaction. Reduction of the severity of this interaction was achieved by redesigning the pod so that the wedge angle was less than the shock detachment angle at the free-stream conditions tested; this resulted in the fluctuating pressure decrease.

Power spectral densities of tested configurations covering a frequency range of 0 to 10 000 cps are illustrated in figure 11. The data used for these plots were the pressure fluctuations measured by transducers 15, 16, 18, and 23, all at $M_0 = 2.0$, and are representative of all data analyzed. Transducers 15, 16, and 18 represent the most active fluctuating pressure instrumentation. Transducer 23 was the least active transducer and is included for reference purposes. The full-length model with the original pod experienced the greatest power at all frequencies for all transducer data analyzed. This power is at a maximum in the low-frequency range below 2000 cps with a peak value of 0.036 pound per square foot squared per cps. The activity tapers off to almost negligible values at 10 000 cps. The shortened model with the original pod illustrates a marked decrease in fluctuating pressure power level when compared with the full-length model. This is particularly true at frequencies below 3000 cps. From 500 to 10 000 cps, the power spectral density of the shortened model did not exceed 0.02 pound per square foot squared per cps. The shortened model with the redesigned pod experienced extremely small pressure fluctuations, as evidenced by the minimal power spectra levels for this configuration over the entire frequency range for all transducer data presented. The greatest amount of fluctuating pressures occurred on the surfaces near the shoulder of the equipment pod.

Flight vehicle frequencies at which considerable power spectra levels were measured have been related to model frequencies by the reduced frequency relation, which is

$$f_m = f_{fs}\left(\frac{D_{fs}}{D_m}\right)\left(\frac{V_m}{V_{fs}}\right)$$

Specific values of interest in this study at Mach 2.0 were full-scale frequencies of 600 and 900 cps and corresponding model frequencies of 5448 and 8172 cps, where the flight and wind tunnel velocities were 1940 and 1762 feet per second, respectively. It is clear from figure 11 that no predominant power spectra levels (high amplitude, narrow band-

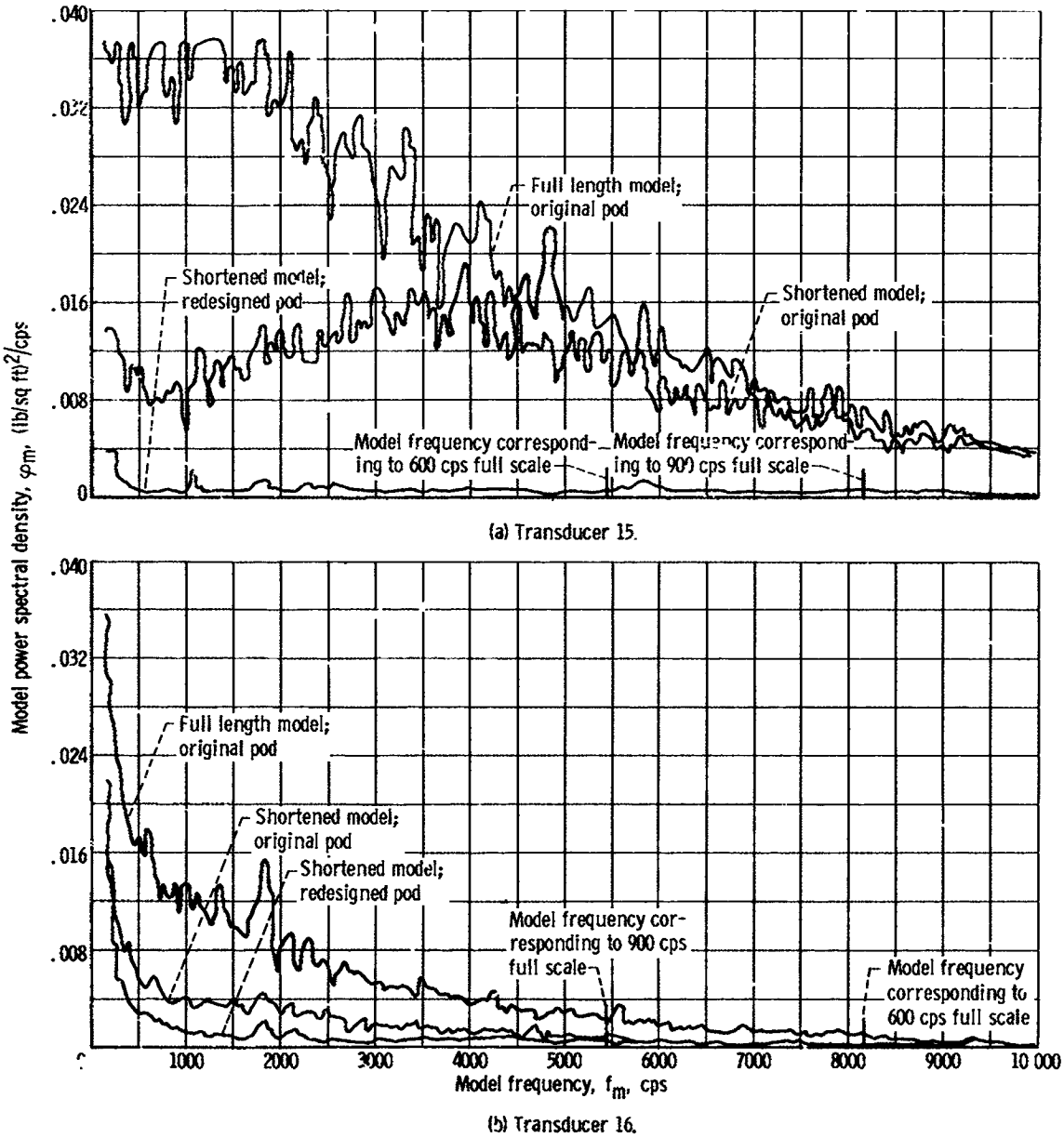

Figure 11. - Power spectral densities of tested configurations at Mach 2.0.

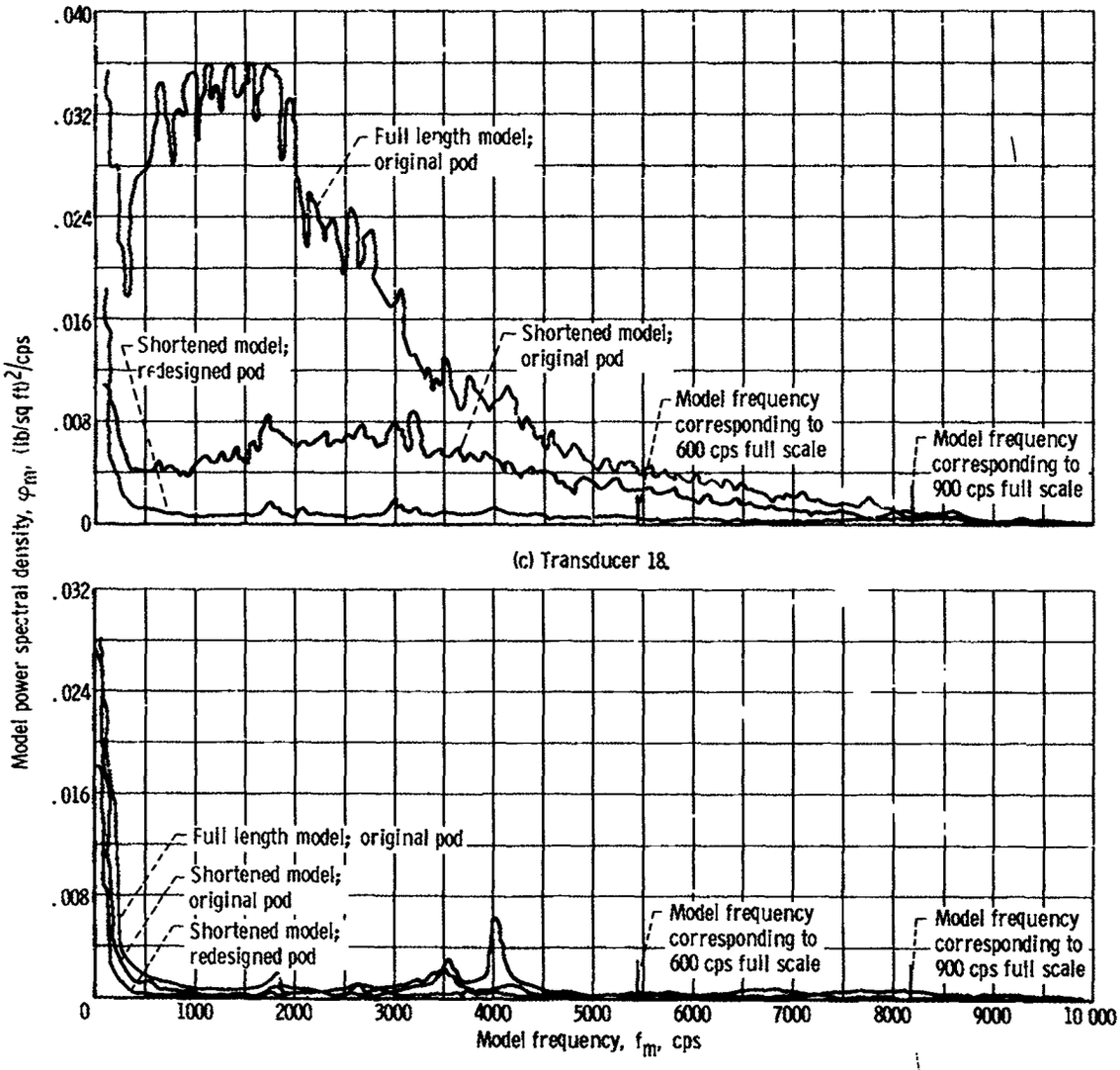

(c) Transducer 18.

(d) Transducer 23.

Figure 11. - Concluded.

width) appeared consistently at either of these frequencies or group of frequencies. This would indicate the possibility that high flight vibration levels at these frequencies may be caused by pressure fluctuations that excite vehicle structures at their natural resonant frequencies. Furthermore, it is felt that the 50 cps bandwidth resolution employed for this 1/10-scale data (comparable to full-scale 5 cps bandwidth) precluded the possibility that the spectrum analyzer averaged out any sharp peaks in pressure fluctuation. It is also evident that the level of pressure fluctuation activity was dependent, to some extent, on boundary-layer effects.

SUMMARY OF RESULTS

A 1/10-scale Atlas-Agena-Mariner C was wind tunnel tested over a Mach number range of 2.0 to 2.5 at an angle of attack of 0°. Attention was centered on the fluctuating pressure activity in the area of an equipment pod. Additional configurations tested were a 1/10-scale model of the Atlas with a shortened nose and the original pod and the same shortened model with a redesigned pod. The following results were obtained:

1. Power spectral densities of the three tested configurations failed to reveal distinct power spectra levels at model frequencies corresponding to full-scale frequencies where significant power concentrations had been observed. This raises the possibility that flight structures are resonating to pressure fluctuations and producing peaks at their natural resonant frequencies.

2. Shock attachment and reduction of shock - boundary-layer interaction reduced the values of the root-mean-square differential pressure coefficients. This was achieved by a redesign of the original pod in which the wedge angle was reduced and the pod lengthened.

3. The use of a short nose on the Atlas considerably reduced the fluctuating pressure levels, possibly because of decreases in shock - boundary-layer interactions that were caused by modifications of boundary-layer profile and thickness.

4. Transducers installed on surfaces in proximity to the equipment pod shoulder measured the highest level of pressure fluctuations.

5. Mach number had little effect on root-mean-square fluctuating pressure values in the Mach number range of 2.0 to 2.5.

Lewis Research Center,
National Aeronautics and Space Administration,
Cleveland, Ohio, May 19, 1966,
493-21-00-01-22.

REFERENCE

1. Anon.: Atlas Launch Vehicle Flight Evaluation Report 250D. Rep. No. GDA/BKF 64-032, General Dynamics Corp., Oct. 30, 1964.

NASA-Langley, 1966 E-3398